

ADVANCED FUNCTIONAL MATERIALS

Supporting Information

for *Adv. Funct. Mater.*, DOI 10.1002/adfm.202309558

Heterogeneous Integration of Graphene and HfO₂ Memristors

*Urška Trstenjak**, *Kalle Goß*, *Alexander Gutsche*, *Janghyun Jo*, *Marcus Wohlgemuth*, *Rafal E. Dunin-Borkowski*, *Felix Gunkel* and *Regina Dittmann**

Supporting Information

Heterogeneous integration of graphene and HfO₂ memristors

Urška Trstenjak^{a,b}, Kalle Goß^{a,c}, Alexander Gutsche^{a,c}, Janghyun Jo^d, Marcus Wohlgemuth^{a,c}, Rafal E. Dunin-Borkowski^d, Felix Gunkel^{a,c}, and Regina Dittmann^{a,c*}

^a Peter Grünberg Institute 7, Forschungszentrum Jülich GmbH, 52428 Jülich, Germany

^b Advanced Materials Department, Jožef Stefan Institute, 1000 Ljubljana, Slovenia

^c Jülich-Aachen Research Alliance (JARA-FIT), 52428 Jülich, Germany

^d Ernst Ruska-Centre for Microscopy and Spectroscopy with Electrons, Forschungszentrum Jülich GmbH, 52428 Jülich, Germany

Keywords: pulsed-laser deposition, quasi van der Waals growth, resistive switching, resistive random-access memory

* Corresponding author.

E-mail address: r.dittmann@fz-juelich.de

Raman measurements of monolayer graphene before deposition

As-transferred monolayer graphene samples were investigated by means of Raman spectroscopy (**Figure S1**). Absence of the *D* band signal, which is induced by defects, attests to the high quality of the as-transferred graphene sample. The intensity ratio of the *2D* and *G* bands offers confirmation that the sample contains single-layer graphene.

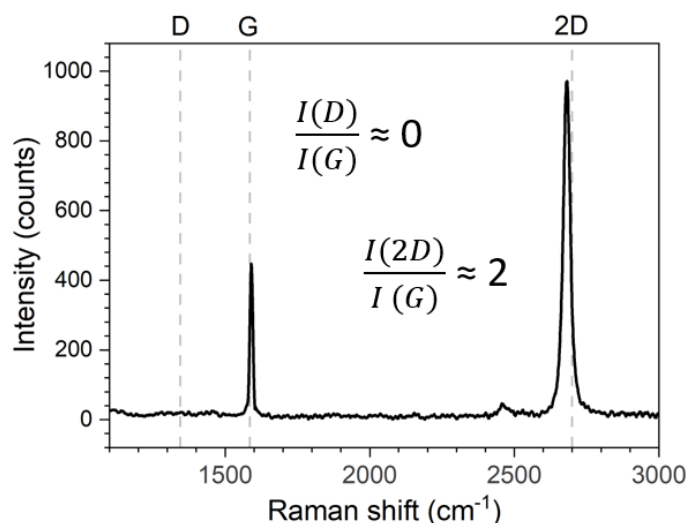


Figure S1: Raman spectrum of an as-transferred monolayer graphene sample on SiO₂/Si.

Parametric series

The Raman spectroscopy results for the target-to-substrate and temperature series are shown in **Figure S2**.

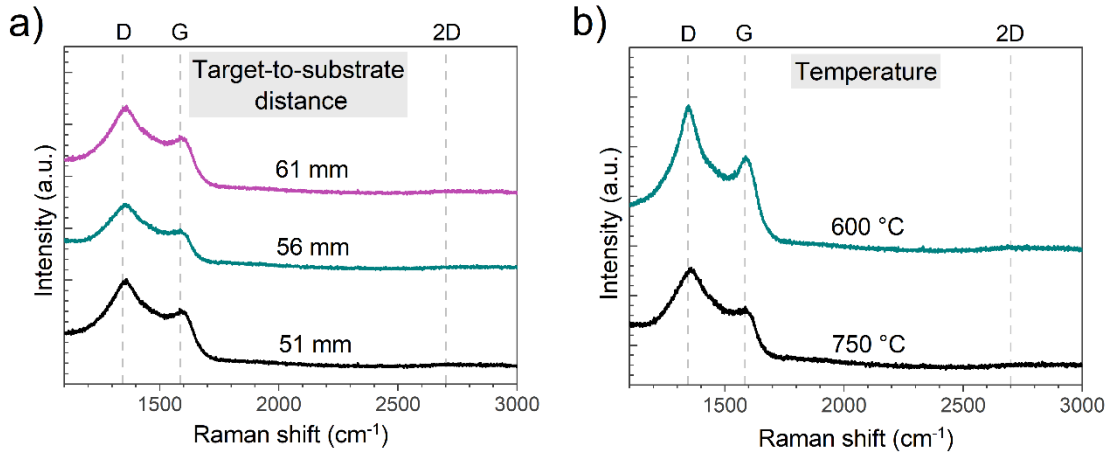


Figure S2: Raman spectra of the samples prepared using different a) target-to-substrate distances and b) deposition temperatures.

The AFM images of the samples grown in different $p(\text{Ar})$ are shown in **Figure S3**.

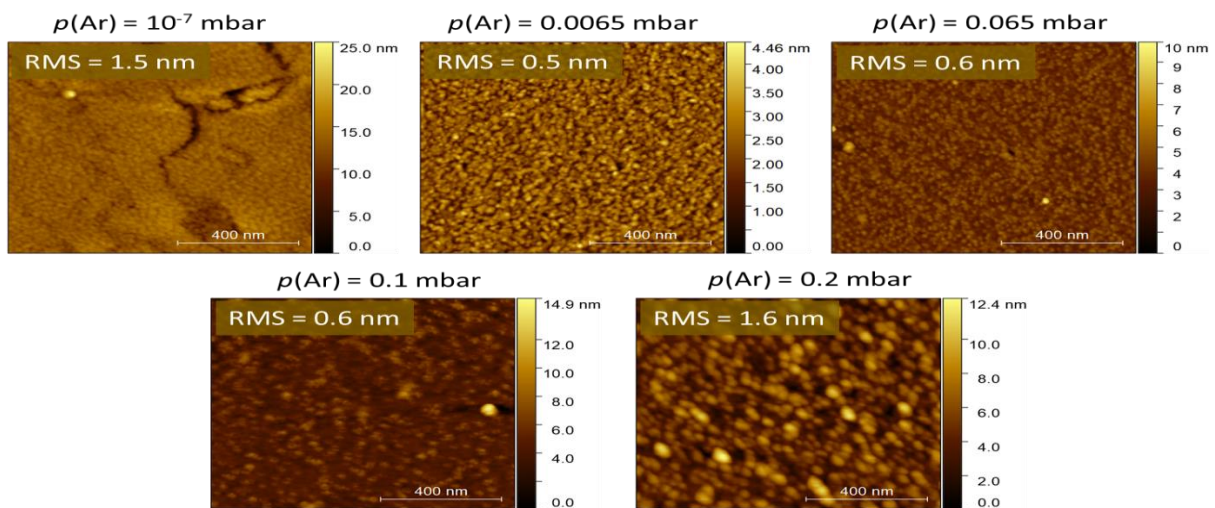


Figure S3: AFM micrographs of the HfO_2 films deposited using varying process pressures.

The results of the Raman investigations of samples grown in different gas atmospheres are shown in **Figure S4**, panel a). Based on the results, the defect density was comparable for the two samples. In panel b), the results of the Raman spectroscopy performed on samples with different cooling rates, is shown. We hypothesized that a faster cooling rate ($80\text{ }^\circ\text{C} / \text{min}$)

could improve the conservation of Gr by reducing the timeframe of the exposure of Gr to oxidative conditions (contact with oxide layers at high temperatures). On the other hand, a slower cooling rate (10 °C / min) could reduce the thermal strain during cool-down, and therefore reduce the mechanical damage to the graphene. The slowly-cooled sample did exhibit a very slightly more pronounced 2D band, and an improved I_D / I_G ratio; however, the full-widths at half maxima (FWHM) of the D and G peaks were broader. Therefore, the defect concentrations in the samples were comparable.

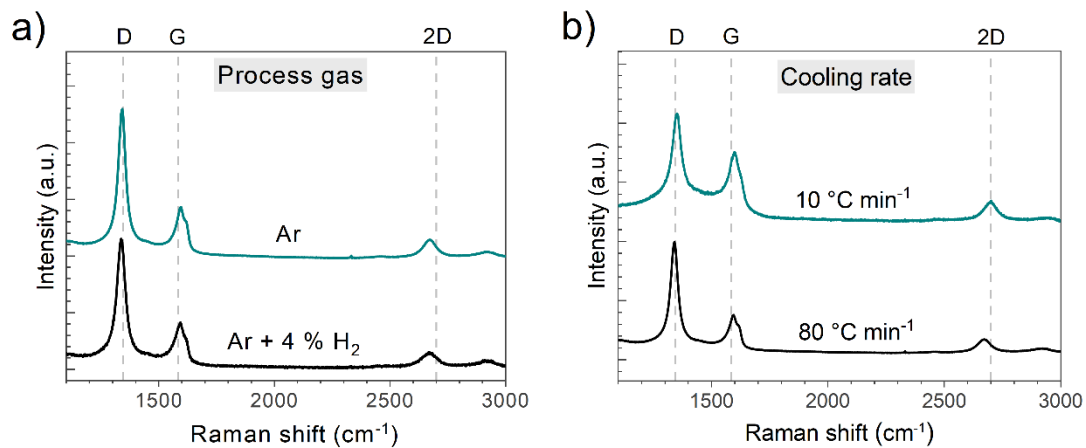


Figure S4: Raman spectra of the samples prepared using different a) process gases and b) cooling rates.

A schematic overview of the influence of various processing parameters on the quality of graphene is shown in **Table S1**. The parameters were varied based on the hypotheses related to a superior conservation of the graphene. The impact on the graphene quality was evaluated based on the approach described in Section 2.3 of the main text, whereas the impact on the oxide film quality was evaluated based on a combination of RHEED, XRD and AFM data.

Table S1: List of PLD parameters, hypotheses and their impact on graphene and HfO₂ quality

Parameter	Hypothesis	Impact on graphene quality	Impact on HfO ₂ quality
<i>Ar pressure</i>	Reduce the kinetic energy of incoming particles	High Higher quality at high pressures	Moderate Slightly higher quality at intermediate pressures
<i>Target-to-substrate distance</i>	Reduce the kinetic energy of incoming particles	Low No significant influence	Low No significant influence

<i>Fluence</i>	Reduce the flux of incoming particles	Moderate Higher quality at lower fluences	Moderate Slightly higher quality at intermediate pressures
<i>Temperature</i>	Suppress chemical reactions at the interface	Low No significant influence	Moderate Slightly higher quality at intermediate pressures
<i>Cooling rate</i>	Suppress chemical interactions at the interface / Reduce thermal strain	Low No significant influence	Low No significant influence
<i>Reducing atmosphere</i>	Prevent oxidation	Low No significant influence	Low No significant influence

Post-annealing

Figure S5 shows the results of Raman spectroscopy of HfO₂ samples grown on ML and BL Gr / SiO₂ / Si after post-annealing in $p(\text{O}_2) = 0.2$ mbar at $T = 750$ °C for $t = 5$ min. The intensity modulation in the ML sample could stem from specific Raman-active species formed at the interface due to oxidation or interdiffusion, which may be less pronounced for the BL sample.

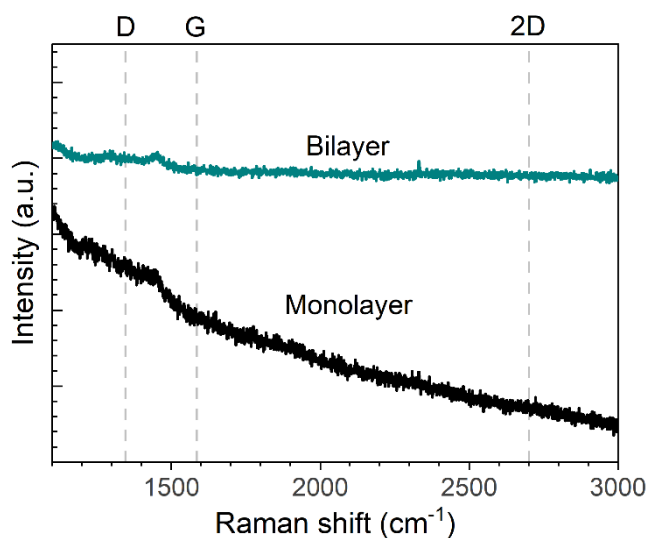


Figure S5: Raman spectroscopy data of post-annealed HfO₂ grown on ML (BL) Gr / SiO₂ / Si.

Cycling behavior

Figure S6 shows the I - V curves of the first 10 cycles on a device with an area of $100 \mu\text{m}^2$ (shown in Figure 8 of the main text). The origin of the observed drift is not clear. We hypothesize that the drift is induced by a predominant oxidation of the HfO_2 during cycling, which might be related to the blocking of oxygen diffusion by the graphene. This might be compensated by using asymmetric biasing schemes in the future.

